ACS OMEGA

Article

Cite This: ACS Omega 2019, 4, 17981−17989

http://pubs.acs.org/journal/acsodf

Pharmacokinetics of the Rac/Cdc42 Inhibitor MBQ-167 in Mice by Supercritical Fluid Chromatography−Tandem Mass Spectrometry

María del Mar Maldonado,[†] Gabriela Rosado-González,[†,§] Joseph Bloom,[‡] Jorge Duconge,[‡] Jean F. Ruiz-Calderón,[†] Eliud Hernández-O'Farrill,[‡] Cornelis Vlaar,[‡] José F. Rodríguez-Orengo,[†,∥] and Suranganie Dharmawardhane*[,†]

[†]Department of Biochemistry and [‡]Department of Pharmaceutical Sciences, School of Pharmacy, University of Puerto Rico Medical Sciences Campus, PO Box 365067, San Juan, Puerto Rico 00936-5067, United States

[§]Department of Biology & Chemistry, University of Puerto Rico Río Piedras, PO Box 23346, San Juan, Puerto Rico 00931-3346, United States

[∥]FDI Clinical Research, 998 Ave. Luis Muñoz Rivera, San Juan, Puerto Rico 00927, United States

Supporting Information

ABSTRACT: The Rho GTPases Rac and Cdc42 are potential targets against metastatic diseases. We characterized the small molecule MBQ-167 as an effective dual Rac/Cdc42 inhibitor that reduces HER2-type tumor growth and metastasis in mice by ∼90%. This study reports the pharmacokinetics and tissue distribution of MBQ-167 following intraperitoneal and oral single-dose administrations. We first developed and validated a bioanalytical method for the quantitation of MBQ-167 in mouse plasma and tissues by supercritical fluid chromatography coupled with electrospray ionization tandem mass spectrometry. MBQ-167 was rapidly distributed into the kidneys after intraperitoneal dosing, whereas oral administration resulted in higher distribution to lungs. The elimination half-lives were 2.17 and 2.6 h for the intraperitoneal and oral dosing, respectively. The relative bioavailability of MBQ-167 after oral administration was 35%. This investigation presents the first analysis of the pharmacokinetics of MBQ-167 and supports further preclinical evaluation of this drug as a potential anticancer therapeutic.

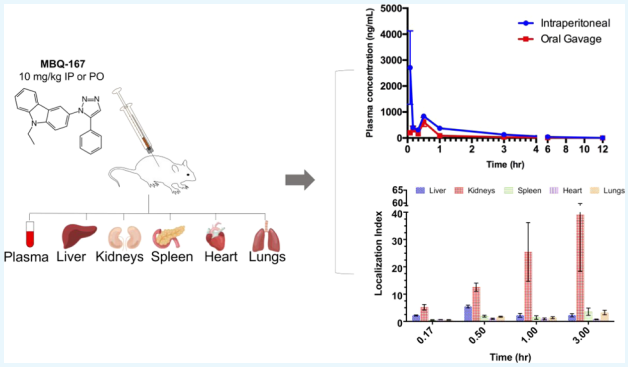

1. INTRODUCTION

The Rho GTPases Rac and Cdc42 regulate cell functions governing metastatic processes such as migration/invasion, tumor growth, angiogenesis, cell cycle progression, and oncogenic transformation. Accordingly, numerous studies have shown that Rac and Cdc42 are hyperactivated in multiple human cancers.[1−4] Hence, targeting of these pivotal regulators is a rational approach for innovative antimetastasis focused therapy design. Recently, we developed the small molecule MBQ-167 as an effective Rac/Cdc42 inhibitor, which is 10 times more potent than other currently available inhibitors, with IC50s of 100 and 80 nM for Rac and Cdc42 activation, respectively.[5,6] MBQ-167 treatment resulted in a decrease in metastatic cancer cell viability and migration in vitro, with concomitant inhibition of signaling to the Rac and Cdc42 downstream effector p21-activated kinase, an oncogene that has been the target of anticancer drug development. In a mouse model of experimental metastasis, MBQ-167 at 10 mg/kg body weight (BW) was effective at reducing HER2-type mammary fat pad tumor growth and metastasis in immunocompromised mice by ∼90 and ∼99%, respectively.[5] Further preclinical efficacy experiments in mouse models of experimental and spontaneous metastasis have demonstrated the utility of MBQ-167 in inhibiting both primary tumor growth and metastasis.

To continue developing MBQ-167 as a potential antimetastatic drug, it is imperative to gather comprehensive information on the pharmacokinetic profile, which would explain the mechanisms of absorption, distribution, metabolism, and elimination of the compound in the body. Moreover, since this compound is a new drug, validated methods for its detection in biological matrixes have yet to be established. Supercritical fluid chromatography coupled with electrospray ionization tandem mass spectrometry (SFC−MS/MS), which uses supercritical carbon dioxide (sCO_2) as the main component of the mobile phase, offers a series of advantages such as rapid analysis times with no reduction in sensitivity or efficiency.[7−11] Recent studies have favorably highlighted this technology for lipophilic compounds when compared to conventional methods like liquid (LC−MS) and gas

Received: June 4, 2019
Accepted: September 24, 2019
Published: October 23, 2019

DOI: 10.1021/acsomega.9b01641
ACS Omega 2019, 4, 17981−17989

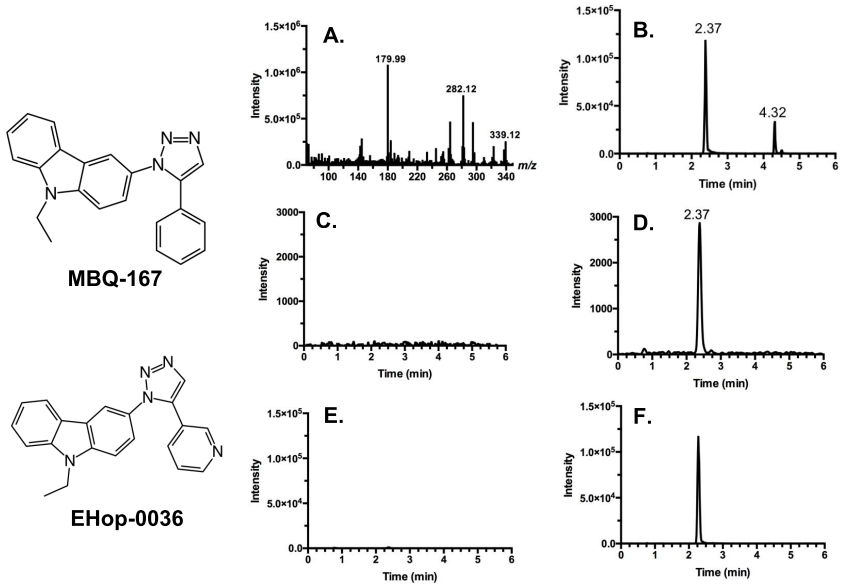

Figure 1. (A) Positive electrospray ionization product ion spectra of MBQ-167. (B) Total ion chromatograms of MBQ-167 (Tr = 2.37 min) and EHop-0036 (Tr = 4.32 min). Multiple reaction monitoring chromatograms (m/z 339.1 > 179.9) of (C) blank plasma sample, (D) MBQ-167 at 1.5 ng/mL in mouse plasma, (E) blank liver sample, and (F) MBQ-167 at 10 ng/mL in the mouse liver.

chromatography (GC−MS).[12,13] Moreover, SFC is an environmentally friendly technique due to its use of less organic solvents. These advantages have rendered SFC-coupled MS/MS as a rapid and sensitive analytical method for pharmacokinetic applications.[14−16]

In this study, we developed and validated an SFC−MS/MS bioanalytical method to quantify the Rac/Cdc42 inhibitor MBQ-167 in mouse plasma and tissues. We applied this method to investigate the pharmacokinetics and tissue distribution in Balb/C mice following a single intraperitoneal (IP) or oral (PO) administration of MBQ-167.

2. RESULTS AND DISCUSSION

2.1. Optimization of Chromatographic and Mass Spectrometry Conditions. The mass spectrometry and chromatographic conditions were first optimized for the analysis of MBQ-167. Figure 1A shows the positive electrospray ionization mass spectrum of MBQ-167, in which the precursor ion of [M + H] + 1 = 339.1 and multiple reaction monitoring (MRM) ions >179.9, 282.1 can be observed in the positive ionization mode. The ion 179.9 was used for quantitative analysis, and the ion 282.1 was used for qualitative analysis. To obtain the highest intensity of fragment ions, the parameters optimized included the electrospray ionization (ESI) source temperature, desolvation temperature, capillary and cone voltage, collision energy, and flow rate of the desolvation gas and cone gas. Mass spectrometry parameters were optimized by direct flow infusion analysis of the MBQ-167 standard solution.

Several ratios of sCO_2 and methanol (MeOH)/0.01% formic acid were used to optimize elution from the chromatographic column (95:5, 96:4, 97:3, v/v), where 95:5 ratio provided the optimum response. A column temperature of 40 °C was selected since it resulted in a better peak shape and a suitable elution time. Other parameters that were optimized included backpressure and isocratic pump flow rate. In addition, the use of 100% methanol as an injection solvent gave the best response when compared to heptane/2-propanol (9:1), acetonitrile (ACN)/methanol (4:1), ethanol 100%, and acetonitrile 100%. Under optimum conditions, MBQ-167 was detected at a retention time of 2.37 min (Figure 1B).

2.2. Optimization of Sample Preparation. We compared several organic solvents and extraction methods to determine the optimal extraction procedure of MBQ-167 from mouse plasma and tissues. In plasma, a greater MBQ-167 recovery was observed after protein precipitation with 100% ACN in comparison with MeOH and a mixture containing MeOH/ACN (1:1). Hence, ACN (100%) was chosen for the plasma extractions since it provided minimal interference, low matrix effects, and high sensitivity. For tissue sample purification, liquid−liquid extraction with a mixture of heptane:ethyl acetate (1:1) resulted in a higher and consistent recovery of MBQ-167 (Figure S1A).

2.3. Internal Standard (IS). After screening various compounds, we selected the small molecule EHop-0036 as an internal standard for method validation because of its structural similarity to MBQ-167 and similar chromatographic properties (Figure 1). Both compounds MBQ-167 and EHop-0036 are 1,5-disubstituted-1,2,3-triazole derivatives with a carbazole moiety at 1-position and an aromatic ring at 5-position. However, the simple phenyl ring at the 5-position in MBQ-167 was replaced with a 3-pyridyl ring in EHop-0036. In addition, EHop-0036 did not interfere with the elution of MBQ-167 (Figure 1B).

2.4. Method Validation. *2.4.1. Selectivity.* We compared the chromatograms of six independent sources of blank mouse plasma with the sample plasma spiked with 1.5 ng/mL MBQ-167 (Figure 1C,D). We observed no significant interferences at the measured mass transition (m/z 339.1 179.9). Similarly, no interferences were seen after the analysis of blank and spiked mouse livers (Figure 1E,F).

2.4.2. Linearity. Linearity was determined for both plasma and liver matrixes. Calibration curves were evaluated using a weighting factor of $1/x$. The dynamic ranges established were 1.5−1000 and 10−1000 ng/mL for mouse plasma and liver, respectively (Figure S2). Linearity was also observed in the

DOI: 10.1021/acsomega.9b01641
ACS Omega 2019, 4, 17981−17989

Table 1. Method Validation for MBQ-167 Quantification in Mouse Plasma and Tissues by SFC-MS/MS

		intraday (n =18)		interday (n = 18)		short term[a] (n = 3)		freeze−thaw (−80 °C, 3 cycles 24 h) (n = 4)		postpreparative (4 °C, 8 h) (n = 6)		long term (−80 °C) (n = 4)			
sample matrix	spiked level (ng/mL)	RSD%	RE%	RSD%	RE%	RSD%	RE%	RSD%	RE%	RSD%	RE%	RSD%	RE%	recovery (%) (n = 6)	matrix effect (%) (n = 6)
plasma	2.5	6.4	8.9	13.5	5.3	6.7	4.0	6.3	−2.7	7.8	8.0	4.3[b]	12.6[b]	53.8	78
	450	10.9	13.2	5.8	−1.9									69.2	96.5
	950	9.6	2.1	13.7	−4.4	14.0	−0.5	13.1	−1.2	3.5	15.2	4.6[d]	−1.0[d]	63.9	94.5
liver	15	6.9	−11.0	11.6	5.2	9.1	0.1	4.4	1.5	6.5	−15	13.6	6.5	73.1	111
	450	6.8	−11.4	11.7	−5.5									60.7	98
	950	7.4	−8.1	6.1	−9.7	6.5	−12.2	7.9	−3.2	0.7	−6.7	12.6	9.2	64.8	94

[a]4 h at a benchtop for plasma; 3 h in an ice bucket for the liver. [b]15 days. [c]90 days at −80 °C for the liver. [d]134 days.

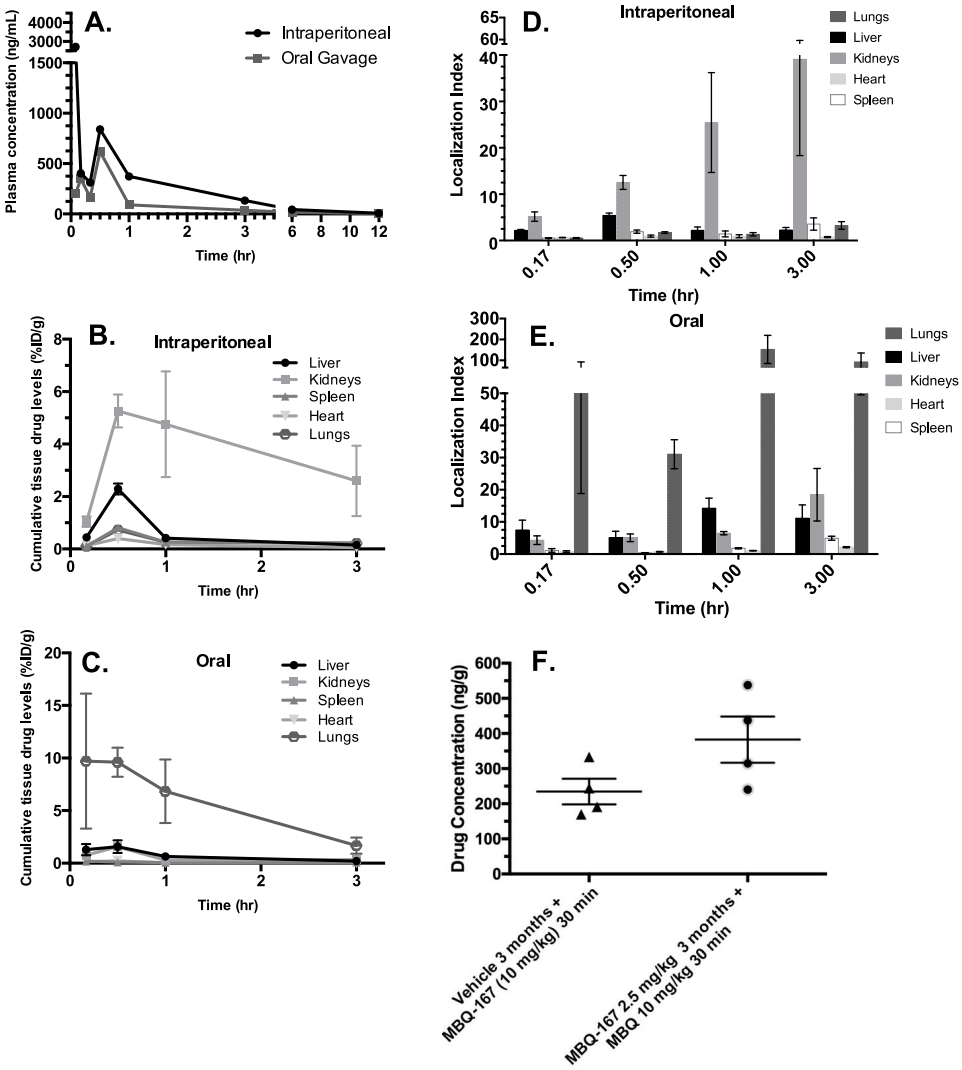

Figure 2. (A) Plasma concentration−time profile of MBQ-167 in Balb/c mice following IP or PO administration. Cumulative tissue MBQ-167 levels as a function of time following (B) ip and (C) po administrations. Tissue localization indexes following (D) IP and (E) PO administrations. (F) Tumor distribution of MBQ-167 from mice that received 2.5 mg/kg BW MBQ-167 three times a week for 3 months, followed by treatment with 10 mg/kg BW MBQ-167 for 30 min, 24 h after the last treatment, or mice treated only with 10 mg/kg BW MBQ-167 for 30 min. Mean standard error of mean (SEM).

same range as liver (10−1000 ng/mL) for kidneys, hearts, and lungs (Figure S2C−E). Our method proved to be highly sensitive for the detection of MBQ-167 in plasma and tissue samples with lower limits of quantification (LLOQ) of 1.5 and 10 ng/mL, respectively. This method has a higher sensitivity in plasma than a UHPLC-MS/MS method that our group previously developed for the detection of EHop-016, which is a

DOI: 10.1021/acsomega.9b01641
ACS Omega 2019, 4, 17981−17989

small molecule Rac inhibitor that shares high structural similarity with MBQ-167.[17]

2.4.3. Accuracy and Precision. We validated the method accuracy and precision for intraday and interday analyses. The intraday and interday accuracy results (relative error, RE%) for MBQ-167 in plasma ranged from 2.1 to 13.2% and 4.4 to 5.3%, respectively. The intraday and interday precision results (relative standard deviation, RSD%) for MBQ-167 in plasma ranged from 6.4 to 10.9% and 5.8 to 13.7%, respectively (Table 1). The validated method was also very accurate and precise for the detection of MBQ-167 in mouse liver, with samples within the acceptable criteria of ±15% (RE and RSD),[18] which indicated that the method was accurate, reliable, and reproducible.

2.4.4. Matrix and Recovery Effects. Plasma and tissues contain a mixture of proteins, carbohydrates, lipids, and other components, which could affect sample quantification, leading to matrix effects. As shown in Table 1, endogenous substances did not significantly interfere with the detection of our drug in plasma and livers since the percent matrix effects ranged from 78 to 96% and 94 to 111% for mouse plasma and liver, respectively. In addition, the observed recovery of MBQ-167 after extraction was consistent, ranging from 52 to 64% in plasma and 60 to 73% in the liver with a coefficient of variation of <15%. As demonstrated in Figure S1B,C, the recovery percent and matrix effect in kidneys, hearts, and lungs are very similar to those in the liver. Hence, the method that was validated for the extraction of MBQ-167 in livers was successfully applied to other organs.

2.4.5. Stability. We investigated the stability of MBQ-167 in mouse plasma and liver under different conditions (Table 1). Results show that MBQ-167 was stable (±15% RSD, RE) in plasma after incubation at ambient temperature for four hours, whereas long-term stabilities at −80 °C were 15 and 134 days for low and high drug concentrations, respectively. Increased drug intermolecular interactions is a possible explanation for greater stability in high-concentration samples since these samples contain a higher number of drug molecules, which could stabilize themselves by interacting with one another. In tissues, MBQ-167 was stable after incubation in an ice bucket for 3 h, whereas the long-term stability at −80 °C was 90 days for both low and high concentrations of quality control samples. For both, plasma and tissues, MBQ-167 was stable after three freeze−thaw cycles lasting 24 h, whereas the postpreparative stability in autosampler conditions was 8 h at 4 °C. These combined results support the robust stability of MBQ-167.

2.5. Plasma Pharmacokinetics. We applied this newly developed and validated SFC-MS/MS method to investigate the pharmacokinetics of MBQ-167 in an in vivo mouse model following intraperitoneal (IP) and per oral (PO) administrations. As shown in Figure 2A, the maximum plasma drug concentration (C_{max}) was 2,969 ng/mL after IP administration. As expected, the plasma drug concentration was lower (∼4.5 times) after PO administration compared to the corresponding dosage given by IP administration. Furthermore, the time-to-peak concentrations were 0.22 and 0.5 h for IP and PO administrations, respectively. MBQ-167 rapid absorption into the bloodstream shows a similar pattern to other previously reported anticancer small molecules.[17,19,20]

The pharmacokinetic profile of MBQ-167 in plasma was evaluated by both compartmental and noncompartmental analyses, and a higher correlation was observed following noncompartmental assessment (Figure S3). Pharmacokinetic parameters corresponding to each average disposition profile are summarized in Table 2. The systemic drug exposures as measured by the area under the curve (AUC_{0-t}) were 1,635 and 585 ng h/mL for IP and PO dosings, respectively. When compared to the related molecule EHop-016, MBQ-167 reached higher plasma peak concentrations (C_{max}) as well as a greater drug exposure (AUC) in both administration routes with the same dose (10 mg/kg BW).[17] The relative bioavailability (F) of MBQ-167 after oral gavage administration was 35%, which is slightly lower than that reported for other anticancer drugs, such as lapatinib (F = 43−50%) and EHop-016 (F = 40%).[17,20] However, other Food and Drug Administration (FDA)-approved small molecules for advanced breast cancer treatment, such as everolimus and paclitaxel, have significantly lower bioavailability (∼5 and ∼11%, respectively).[21−23]

Table 2. Plasma Pharmacokinetics of MBQ-167 (Mean± SEM)

	intraperitoneal	oral gavage
AUC_{0-t} (h ng/mL)	1635 ± 291	585 ± 150
T_{max} (h)	0.22 ± 0.14	0.5 ± 0.0
C_{max} (ng/mL)	2969 ± 1384	619 ± 195
K_{el}(h^{-1})	0.320 ± 0.009	0.27 ± 0.02
$T_{1/2}$ (h)	2.17 ± 0.06	2.6 ± 0.2
V_z/F (mL)	399 ± 63	1403 ± 292
Cl/F (mL/h)	129 ± 24	390 ± 111
MRT INF (h)	1.9 ± 0.1	1.9 ± 0.1
F (%)		35 ± 3

The elimination half-lives ($t_{1/2}$) were 2.17 h for IP dosing and 2.6 h for PO administration. The mean residence time (MRT) and elimination half-life values of MBQ-167 show relatively rapid elimination of this drug from mouse plasma. These results are consistent with other reports of Rac inhibitors being rapidly eliminated from plasma.[17,24] For example, the $T_{1/2}$ of the Rac inhibitor EHT1864 is 1.65 h, which is less than the 2.17−2.6 h $T_{1/2}$ of MBQ-167.[24] Rapid systemic clearances of the drug were also observed with a similar range for both routes of administration (129 and 390 mL/h for IP and PO, respectively). Once adjusted by the corresponding F value, both the volume of distribution (491 mL) and systemic clearance (136.5 mL/h) of MBQ-167 after PO administration nearly resembled those for the IP input. Notably, the systemic clearance of MBQ-167 was estimated to be ∼5 L/(h kg) (i.e., 130 mL/h in a mouse weighing 20−25 g), which exceeds the mean basal renal glomerular filtration rate in mice (i.e., ∼7−11 μL/(min g) or 12−18 mL/h) by ∼10-fold. This clearance rate is ∼85% of the liver blood flow in the mouse. Taken together, these values suggest that MBQ-167 may be removed from the mouse by a combination of elimination mechanisms that include both renal and hepatic pathways.

The volumes of distribution (V_z/F) of MBQ-167 were 399 and 1403 mL for ip and po administrations, respectively. Given an estimated total blood volume of 1.5−2.0 mL in a mouse of 20−25 g, the "apparent" volume of distribution of MBQ-167 in mice (∼400 mL) suggests there was a substantial binding or penetration of this drug into peripheral tissues with less than 1% remaining in the bloodstream.

DOI: 10.1021/acsomega.9b01641
ACS Omega 2019, 4, 17981−17989

Table 3. Pharmacokinetic Parameters Following Intraperitoneal (IP) Administration of 10 mg/kg of MBQ-167 (Mean±SEM)

	heart	kidneys	liver	lungs	spleen
AUC_{0-t} (h %ID/g)	0.46 ± 0.14	16.3 ± 7.2	3.9 ± 1.3	0.86 ± 0.20	1.4 ± 0.5
T_{max} (h)	0.5 ± 0.0	0.67 ± 0.17	0.5 ± 0.0	0.5 ± 0.0	0.5 ± 0.0
C_{max} (%ID/g)	0.40 ± 0.11	6.00 ± 1.40	2.3 ± 0.2	0.72 ± 0.08	0.81 ± 0.16
K_{el} (h^{-1})	0.74 ± 0.08	0.50 ± 0.03	0.50 ± 0.27	0.39 ± 0.05	0.37 ± 0.02
$T_{1/2}$ (h)	0.97 ± 0.12	1.39 ± 0.08	2.24 ± 0.81	1.84 ± 0.24	1.89 ± 0.11
V_z/F (mL)	334 ± 139	23 ± 12	70 ± 9	201 ± 38	268 ± 135
Cl/F (mL/h)	224 ± 66	12 ± 7	31 ± 13	82 ± 26	93 ± 42
MRT INF (h)	0.98 ± 0.01	2.12 ± 0.07	3.56 ± 0.83	1.27 ± 0.06	2.00 ± 0.08

Table 4. Pharmacokinetic Parameters Following Oral Gavage (PO) Administration of 10 mg/kg of MBQ-167 (Mean ±SEM)

	heart	kidneys	liver	lungs	spleen
AUC_{0-t} (h %ID/g)	0.22 ± 0.03	2.5 ± 0.9	4 ± 2	17 ± 7	1.5 ± 0.2
T_{max} (h)	0.5 ± 0.0	0.5 ± 0.0	0.5 ± 0.0	0.28 ± 0.11	4.1 ± 1.9
C_{max} (%ID/g)	0.22 ± 0.03	1.6 ± 0.4	1.6 ± 0.7	13 ± 5	0.26 ± 0.06
K_{el} (h^{-1})	0.52 ± 0.01	0.24 ± 0.08	0.43 ± 0.10	0.87 ± 0.22	0.08 ± 0.03
$T_{1/2}$ (h)	1.34 ± 0.03	3.4 ± 0.9	1.9 ± 0.6	0.89 ± 0.18	11 ± 3
V_z/F (mL)	674 ± 101	188 ± 35	135 ± 108	10 ± 4	535 ± 42
Cl/F (mL/h)	347 ± 44	51 ± 25	37 ± 23	10 ± 6	44 ± 16
MRT INF (h)	1.03 ± 0.05	2.7 ± 0.5	5 ± 1	0.89 ± 0.08	5.7 ± 0.2

2.6. Tissue Distribution. Concentrations of MBQ-167 were determined in the liver, lung, spleen, kidneys, and heart from BALB/c mice at different postdose time points. Figure 2B,C shows the cumulative tissue drug levels over time, following IP or PO administration of MBQ-167. After IP administration, the highest concentrations of MBQ-167 were detected in kidneys, reflecting a pivotal role of renal uptake and subsequent clearance in drug disposition. Figure 2D,E shows the tissue localization index, as determined by the ratio of cumulative levels of MBQ-167 found in tissues when compared to plasma. At 3 h postintraperitoneal dose, MBQ-167 was detected in the kidneys at a ∼40 times higher concentration than in plasma. Although IP administration is expected to bypass the first-pass liver extraction, similar levels of MBQ-167 and their corresponding hepatic distribution patterns were observed after both IP and PO administrations, indicating that hepatic metabolism is also involved.

As expected, the oral gavage group showed a different pattern of distribution, where MBQ-167 is absorbed from the GI tract and passed through the portal-hepatic vein system into the liver for processing before reaching the systemic circulation. In the case of oral administration of MBQ-167, a higher distribution was observed in the lungs, peaking at 0.5 h following administration (Figure 2D). As shown in Figure 2E, the amount of MBQ-167 detected in the lungs was significantly higher than in plasma at similar times. This difference and high variability can be due to the route of administration. In our study, the mice were fed ad libitum before oral gavage, which could have caused differences in the stomach contents at the time of dosing, increasing their risk for gavage-related reflux and aspiration of the drug formulation, as previously reported in rodents.[25] Nonetheless, high AUC in the lungs after oral gavage in mice has also been observed with other FDA-approved small molecules used for breast cancer treatment, such as lapatinib.[26]

Tables 3 and 4 summarize the pharmacokinetic tissue distribution parameters of MBQ-167 for IP and PO dosing, respectively, after noncompartmental analysis (NCA). For IP, the rank order of tissue drug exposure, as determined by AUC, was kidney> liver> spleen> lung> heart, and a similar pattern was observed for maximum MBQ-167 concentration (Cmax) (Table 3). Half-lives of MBQ-167 ranged from 0.97 ± 0.12 h in the heart to 2.24 ± 0.81 h in the liver. For PO, higher MBQ-167 exposure was seen in the lungs, followed by liver, kidneys, spleen, and heart. Half-lives ranged from 0.89 ± 0.18 h (lungs) up to 11 ± 3 h (spleen) (Table 4).

2.7. MBQ-167 Tumor Distribution. To determine MBQ-167 distribution to tumors, mammary fat pad tumors were established from the MDA-MB-468 triple-negative breast cancer cell line in SCID mice. Following tumor homogenization and purification, MBQ-167 was detected by our method in only the two subgroups (n = 5) that received the drug 30 min prior to sacrifice (Figure 2F). The MBQ-167 concentration was slightly higher in the subgroup that received multiple low doses of MBQ-167 (2.5 mg/kg BW) over 3 months followed by 10 mg/kg BW MBQ-167 30 min prior to sacrifice (382.5 ng/g± 59; mean ±SEM) compared to the single-dose subgroup (234.6 ng/g± 33). The amount of MBQ-167 detected in tumors in the single-dose subgroup was lower than the mean drug concentration in plasma (839.92 ng/mL), liver (4565 ng/g), kidneys (10,528.72 ng/g), heart (796.96 ng/g) spleen (1622 ng/g), and lungs (14,46.88 ng/g) at 30 min postdose via IP (Figure S4). Even though tumor drug levels were below those seen in plasma and other tissues, previous studies have demonstrated that the plasma concentration does not necessarily correlate with the antitumor effect. For example, in a study with 5-fluorouracil, tumor levels were below those observed in plasma and it was noted that these amounts could not be correlated with the antitumor effect of the drug.[27]

As expected, MBQ-167 was not detected in the subgroup that received only the vehicle treatments. The drug was also not detected in the subgroup that received 2.5 mg/kg BW MBQ-167 24 h prior to sacrifice, as part of a 3-month regimen of multiple low-dose inputs. This is not surprising because MBQ-167 was eliminated from plasma and tissues ∼6−8 h

DOI: 10.1021/acsomega.9b01641
ACS Omega 2019, 4, 17981−17989

following administration by both routes. Nonetheless, the administration of MBQ-167 three times a week for ∼60 days still significantly reduces tumor growth and metastasis in immunocompromised mice bearing tumors from human breast cancer cells, as previously published by our group.[5] Further studies are needed to characterize the tumor pharmacokinetics of MBQ-167 and to determine the exact length of time that MBQ-167 remains in tumors after administration.

3. CONCLUSIONS

The Rho GTPases, Rac and Cdc42, are viable antimetastatic cancer targets since their activation promotes survival, proliferation, and invasion/migration of cancer cells.[4] So far, no dual or single Rac/Cdc42 inhibitors have entered clinical trials.[28] However, the dual Rac/Cdc42 inhibitor MBQ-167 shows promise as an antimetastatic breast cancer compound by inhibiting tumor growth and metastasis in mouse models.[5] The aim of this study was to elucidate the pharmacokinetics of the dual Rac/Cdc42 inhibitor MBQ-167, which is imperative for dose regimen design and further development of clinical trials. We developed a rapid, sensitive, and selective supercritical fluid chromatography−tandem mass spectrometry method for the detection of MBQ-167 in mouse plasma and tissues. This is the first analytical method that has been developed for the detection of MBQ-167 in a biological matrix and successfully applied in a pharmacokinetic study. This drug is highly distributed to tissues and rapidly eliminated; hence, strategies to optimize drug formulation to increase the drug half-life should be considered in future studies.

4. EXPERIMENTAL SECTION

4.1. Materials. Organic LC/MS-grade solvents acetonitrile (ACN) and methanol (MeOH) were purchased from Sigma-Aldrich (Saint Louis, MO). Sodium chloride, ethyl acetate, heptane, and all materials required for compound synthesis were also purchased from Sigma-Aldrich (Saint Louis, MO). Formic acid was purchased from Fisher (Fair Lawn, NJ). Nonsterile mouse plasma containing sodium citrate was from Equitech-Bio, Inc (Kerrville, TX). Mouse livers used in method validation were obtained from Jackson Laboratory (Bar Harbor, ME). MBQ-167 and EHop-0036 (Figure 1) were used as analytical standards, and MBQ-167 was synthesized as previously described by us.[5] The synthesis of EHop-0036 is described in Figure S5. Purity (>98%) was verified by thin layer chromatography, NMR spectroscopy, and gas chromatography/mass spectrometry (GC/MS).

4.2. Instrumentation. The analysis was performed on an Acquity UPC^2 system (Waters Corp., Milford, MA), coupled to a triple quadrupole MS/MS. The separation was performed on an Acquity UPC^2 BEH (3.0 × 100 mm^2, 1.7 μm) with sCO_2 and methanol/0.01% formic acid as the mobile phase at a rate of 1.0 mL/min, whereas 0.01% formic acid in methanol was used as the makeup solvent at a flow rate of 0.15 mL/min. The gradient elution of A (sCO_2) and B (methanol/0.01% formic acid) was performed as follows: 5% B maintained at 0−1.5 min, 5−12% B at 1.5−2 min, 12% B at 2−3 min, 12−20% B at 3−3.5 min, 20% B at 3.5−4.5 min, 20−5% B at 4.5−5 min, and 5% B at 5−6 min. The backpressure of the system was kept at 2200 psi, and the column temperature was maintained at 40 °C. The autosampler was conditioned at 4 °C. The total run time for analysis was 6 min, and the injection volume was 1.0 μL.

The mass analysis and detection were conducted using a Waters ACQUITY Tandem Quadrupole Detector (TQD) (Waters Corp., Milford, MA) with an ESI interface. The ESI source was operated in the positive ionization mode. The source temperature was set at 150 °C, and the desolvation temperature was kept at 200 °C, whereas the capillary voltage was 3.90 kV for MBQ-167 and the Internal Standard (IS) EHop-0036. The cone voltage was maintained at 66.0 V for MBQ-167 and 42.0 V for the IS. The collision energies of MBQ-167 and IS were 32.0 and 16.0 V, respectively. The cone flow and nitrogen flow rates were set at 1 and 650 L/h, respectively, and instrument control and data acquisition were carried out using MassLynx software with a TargetLynx program (Waters Corp., Milford, MA). MBQ-167 with a precursor ion $[M + H]^+$ = 339.12 and EHop-0036 with a precursor ion $[M + H]^+$ = 340.1 were used as analytical standards monitoring the multiple reaction monitoring (MRM) transitions $[M + H]^+$ = 339.12 > 179.9 and 339.12 > 282.1 for MBQ-167 and $[M + H]^+$ = 340.14 > 312.8 for EHop-0036, respectively. The analysis required the ratio between the quantitative ion (179.9) and the qualifier ion (282.1) of MBQ-167 to be within ±10% to meet the criterion for a positive result. Nitrogen (99.95%) was used as a sheath gas.

4.3. Plasma Sample Extraction. Plasma samples were extracted by a standard protein precipitation method (Figure S6A). A total of 200 μL of plasma was transferred to a 1.5 mL Eppendorf tube. When appropriate, 50 μL of the internal standard (from working solution 2000 ng/mL prepared in 4:1 ACN:MeOH) was added to the sample. Proteins in the matrix were precipitated by the addition of 550 μL of cold ACN and vortexed for 10 min using a VWR Analog Vortex Mixer. Samples were then centrifuged for 10 min at 1000*g* at 4 °C using a VWR Galaxy 16 microcentrifuge. The supernatant was collected and dried using a Labconco Centrivap console. Dried samples were reconstituted by adding 200 μL of 100% MeOH solution, vortexed for 10 min, and centrifuged at 1000*g* for 1 min. Samples were transferred to autosampler vials, sealed, and injected onto the UPC^2 system.

4.4. Tissue Sample Extraction. Tissue samples were extracted by the liquid−liquid extraction method (Figure S6B). Stored organs were thawed, weighed (100 mg), and homogenized using the Polytron PT 2100 instrument in pH 7.4 saline (1:4 w/v).[29] Similarly to refs,[30,31] the tissue homogenate (100 μL) was transferred to another tube, followed by addition of the internal standard (10 μL from 4500 ng/mL stock), and vortexed for 30 s. Subsequently, 100 μL of NaOH 0.5 M was added to the mixture and vortexed for 5 min. A liquid−liquid extraction was performed using 790 μL of heptane/ethyl acetate (1:1). Samples were then vortexed for 10 min and later centrifuged for 5 min at 510*g*. The upper layer was recovered, and the solvent was evaporated for one hour in a Labconco Centrivap console at room temperature. Afterward, samples were reconstituted with 100 μL of methanol, vortexed for 10 min, and centrifuged at 1000*g* for 1 min. Samples were then transferred to an autosampler vial to be analyzed by SFC-MS/MS.

4.5. Method Validation. This method was validated following the US Food and Drug Administration (FDA) Bioanalytical Method Validation Guide.[18]

4.5.1. Preparation of Standard Solutions, Plasma and Tissue Calibrators, and Quality Controls. A primary stock solution of the MBQ-167 analyte (2 mg/mL) was prepared by

DOI: 10.1021/acsomega.9b01641
ACS Omega 2019, 4, 17981−17989

dissolving 10 mg of the analyte in an acetonitrile:methanol (4:1) mixture. A stock solution of the EHop-0036 internal standard (2 mg/mL) was prepared in the same manner. Analyte stock solutions were stored in the dark at −20 °C. The internal standard EHop-0036 working solutions (2000 and 4500 ng/mL) were prepared from a 20 000 ng/mL stock in an acetonitrile:methanol (4:1) mixture. Working solutions of MBQ-167 in methanol were prepared using 20 000 and 50 000 ng/mL stock solutions.

For plasma, calibration curves were prepared using working solutions of MBQ-167 at 1.5, 5, 25, 100, 350, 500, and 1000 ng/mL in mouse plasma. Standard solutions were prepared by diluting primary stock solutions in mouse plasma. Quality control (QC) samples were prepared using working solutions to obtain the desired concentrations of 2.5, 450, and 950 ng/mL. Plasma samples were prepared individually by adding 50 μL of internal standard (from working solution 2000 ng/mL) to 200 μL of plasma solution spiked with MBQ-167, followed by extraction, as described above.

For tissues, calibration curves were prepared using 10, 20, 40, 62.5, 125, 250, 500, and 1000 ng/mL of MBQ-167. Standard solutions were prepared by diluting primary stock solutions in methanol. QC samples were prepared using working solutions to obtain the desired concentrations of 15, 450, and 950 ng/mL. Each tissue sample was prepared by adding 10 μL of the corresponding MBQ-167 stock solution in methanol and 10 μL of the internal standard (from 4500 ng/mL stock) to 100 μL of the tissue homogenate, followed by extraction, as described above.

4.5.2. Accuracy and Precision. The intraday precision and accuracy were measured by comparing three calculated QC concentrations (six replicates per concentration level) against their nominal concentrations in one batch. The interday precision and accuracy were measured by comparing the three calculated QC concentrations (six replicates per concentration level) from three independent batches run on separate days. The accuracy and precision of the method were described by percent relative error (RE%) and relative standard deviation (RSD%), respectively. The lower limit of quantification (LLOQ) was defined as the lowest concentration that could be determined with both RE and RSD within ±20%.

4.5.3. Selectivity. Selectivity was evaluated using six independent sources of blank mouse plasma and blank mouse tissue and the resulting chromatograms compared with plasma and tissue samples spiked with MBQ-167 at the LLOQ.

4.5.4. Recovery and Matrix Effects. The recovery of MBQ-167 was measured in spiked mouse plasma and tissue at three QC concentrations based upon six replicates and compared to that of MBQ-167 in 100% methanol at the same concentrations. Recovery was calculated by comparing the peak areas of blank biological samples spiked before extraction to those of the samples in which the analyte was added after extraction. The matrix effect was evaluated by comparing the peak areas of the blank matrix spiked after extraction to those of pure standard solutions.

4.5.5. Stability. MBQ-167 stability in plasma and tissues was measured under several storage conditions. For plasma, the short-term stability (2.5 and 950 ng/mL) was evaluated for 4 h at room temperature. The postpreparation response of the three QC concentrations was determined after 10 h at 4 °C. The long-term stability was evaluated after storing the samples at −80 °C after 15 and 134 days.

For tissues, the short-term stability was evaluated by leaving the QC samples with the lowest and highest concentrations (15 and 950 ng/mL) at a benchtop for 3 h in an ice bucket. The postpreparative stability for the three QC concentrations (15, 450, and 950 ng/mL) was determined after 8 h at 4 °C. The long-term stability was evaluated after storing the samples at −80 °C after 90 days. The freeze−thaw stability at −80 °C was evaluated for three 24 h cycles.

4.6. Animal Protocol. All experimental procedures were conducted under an approved protocol #A8180117 by The University of Puerto Rico Medical Sciences Campus Institutional Animal Care and Use Committee (IACUC), in accordance with the principles and procedures outlined in the NIH Guideline for the Care and Use of Laboratory Animals.[32] Four to five-week-old female BALB/c mice (Charles River Laboratories, Inc. Wilmington, MA) were housed under pathogen-free conditions in HEPA-filtered cages and kept on a 12 h light/dark cycle and controlled temperature (22−24 °C) and humidity (25%). Food and water were given ad libitum. After one-week acclimation, animals were treated with MBQ-167. MBQ-167 was prepared as a stock solution of 2 mg/mL in cremophor/ethanol/PBS (12.5:12.5:75) solution. A total of 90 BALB/c mice were used in the pharmacokinetic study, with five mice per group.

4.6.1. Pharmacokinetic Study. For the analysis of MBQ-167 bioavailability, each mouse was administered a single 0.1 mL dose of MBQ-167 (in 12.5% ethanol, 12.5% cremophor, 75% phosphate-buffered saline, pH 7.4) that corresponded to 10 mg/kg by IP injection or oral gavage (PO). Following treatment, five mice per group were sacrificed by cervical dislocation at 0.08, 0.17, 0.33, 0.5, 1, 3, 6, and 12 h. Blood (∼1.0 mL) was rapidly collected by cardiac puncture exsanguination and transferred into sodium citrate buffer tubes on ice. After centrifuging at 16 000*g* for 20 min at 4 °C, plasma was then recovered and stored at −80 °C until analysis. The livers, heart, spleen, kidneys, and lungs were rapidly collected from each animal at different time points (0.17, 0.5, 1, and 3 h after drug administration), flushed with normal saline, individually wrapped in an aluminum foil, snap-frozen in liquid nitrogen, and stored frozen at −80 °C until use. The time intervals for collecting tissues were shorter than those for the plasma collections because we wanted to ascertain the tissue distribution of MBQ-167 in a broad and humane fashion while sacrificing a minimal number of mice.

4.6.2. Distribution of MBQ-167 in Mouse Mammary Tumors. A total of 20 female SCID mice (Charles River Laboratories, Inc. Wilmington, MA), 4-week-old, were injected with 2×10^6 green fluorescent protein (GFP)-tagged MDA-MB-468 human breast cancer cells at the mammary fat pad under isoflurane inhalation (1−3% in oxygen using an inhalation chamber at 2 L/min) to produce primary tumors, as described.[33] After tumor establishment (1 week later), 10 mice per group were treated with either vehicle or MBQ-167 (2.5 mg/kg) via intraperitoneal (ip) injections, three times a week for 3 months. After 24 h of the last treatment, a single dose of MBQ-167 (10 mg/kg BW) was administered to five mice from the vehicle group and five mice of the treated group for 30 min prior to sacrifice. Following sacrifice, tumors were flushed with normal saline, individually wrapped in an aluminum foil, snap-frozen in liquid nitrogen, and stored frozen at −80 °C until use.

4.6.3. Pharmacokinetics and Tissue Distribution Data Analysis. All experimental data were expressed as a mean from

DOI: 10.1021/acsomega.9b01641
ACS Omega 2019, 4, 17981−17989

five animals per each time-point. Data analysis was performed by noncompartmental analysis (NCA), according to a uniform weighing scheme, using Phoenix WinNonlin professional software, Version 8.1 (Certara Inc., 2018, NJ). The area under the curves (AUCs) for the tissue or plasma concentrations over time were determined using the linear−log linear trapezoidal rule. The largest adjusted regression was selected to estimate lambda z, with one caveat: if the adjustment did not improve, but was within 0.0001 of the largest value, the regression with a larger number of points was used. Lambda *z* is the first-order rate constant associated with the terminal (log linear) segment of the curve, as estimated by linear regression. Parameters extrapolated to infinity using the moments of the curves were all computed based on the last predicted value. We calculated the mean percentage of injected dose per gram of tissue [%ID/g] at the time points indicated above. To this purpose, a standard dose was used to determine 100% (total) amount of entire dose administration. The corresponding indexes of localization (IL) were calculated as the tissue-to-plasma ratios of the previously calculated %ID per gram of tissue and per milliliter of plasma.

■ ASSOCIATED CONTENT

Supporting Information

The Supporting Information is available free of charge on the ACS Publications website at DOI: 10.1021/acsomega.9b01641.

Method development of liquid−liquid extraction in tissues (Figure S1); calibration curves of MBQ-167 in biological matrixes (Figure S2); pharmacokinetic profile curves (Figure S3); tissue concentration−time profile of MBQ-167 (Figure S4); design and synthesis of EHop-0036 (Figure S5); extraction of MBQ-167 from biological matrixes (Figure S6) (PDF)

■ AUTHOR INFORMATION

Corresponding Author

*E-mail: su.d@upr.edu. Tel: 787-758-2525X1630.

ORCID

María del Mar Maldonado: 0000-0001-6847-2707

Notes

The authors declare no competing financial interest.

■ ACKNOWLEDGMENTS

This work was supported by NIGMS-RISE R25 GM061838 (to M.D.M.); NIH/NIMHD U54 MD007600-31 (to J.D.); NIH/NIGMS P20 GM103475-15 (to J.F.R.-C.); Puerto Rico Science, Technology and Research Trust, NIH/NIGMS SC3 GM084824 and Susan Komen for the Cure OGI 70023 (to S.D.); and MARC (NIH/NIGMS 5T34GM007821-39) (to G.R.-G.). We would like to thank Dr. Valance Washington for providing us with mouse plasma and Raúl Blanco for his assistance and training for the Waters UPC^2-MS/MS. We also want to thank Dr. Linette Castillo-Pichardo and Ailed Cruz for assistance with oral gavage. Finally, we thank Dr. Edwin O. Ortiz-Quiles for providing valuable technical feedback in the analytical method development and validation.

■ REFERENCES

(1) Kazanietz, M. G.; Caloca, M. J. The Rac GTPase in Cancer: From Old Concepts to New Paradigms. *Cancer Res.* **2017**, *77*, 5445−5451.

(2) Stengel, K.; Zheng, Y. Cdc42 in Oncogenic Transformation, Invasion, and Tumorigenesis. *Cell Signal.* **2011**, *23*, 1415−1423.

(3) Maldonado, M. dei M.; Dharmawardhane, S. Targeting Rac and Cdc42 GTPases in Cancer. *Cancer Res.* **2018**, *78*, 3101 LP−3111.

(4) Porter, A. P.; Papaioannou, A.; Malliri, A. Deregulation of Rho GTPases in Cancer. *Small GTPases* **2016**, *7*, 123−138.

(5) Humphries-Bickley, T.; Castillo-Pichardo, L.; Hernandez-O'Farrill, E.; Borrero-Garcia, L. D.; Forestier-Roman, I.; Gerena, Y.; Blanco, M.; Rivera-Robles, M. J.; Rodriguez-Medina, J. R.; Cubano, L. A.; Vlaar, C. P.; Dharmawardhane, S. Characterization of a Dual Rac/Cdc42 Inhibitor MBQ-167 in Metastatic Cancer. *Mol. Cancer Ther.* **2017**, *16*, 805−818.

(6) Rivera-Robles, M. J.; Medina-Velazquez, J.; Asencio-Torres, G. M.; Gonzalez-Crespo, S.; Rymond, B. C.; Rodriguez-Medina, J.; Dharmawardhane, S. Targeting Cdc42 with the Anticancer Compound MBQ-167 Inhibits Cell Polarity and Growth in the Budding Yeast S. Cerevisiae. *Small GTPases* **2018**, 1−11.

(7) Kalíková, K.; Šlechtová, T.; Vozka, J.; Tesařová, E. Supercritical Fluid Chromatography as a Tool for Enantioselective Separation; A Review. *Anal. Chim. Acta* **2014**, *821*, 1−33.

(8) Li, F.; Hsieh, Y. Supercritical Fluid Chromatography-Mass Spectrometry for Chemical Analysis. *J. Sep. Sci.* **2008**, *31*, 1231−1237.

(9) Matsubara, A.; Fukusaki, E.; Bamba, T. Metabolite Analysis by Supercritical Fluid Chromatography. *Bioanalysis* **2010**, *2*, 27−34.

(10) Pilařová, V.; Plachká, K.; Khalikova, M. A.; Svec, F.; Nováková, L. Recent Developments in Supercritical Fluid Chromatography − Mass Spectrometry: Is It a Viable Option for Analysis of Complex Samples? *TrAC, Trends Anal. Chem.* **2019**, *112*, 212−225.

(11) Dispas, A.; Jambo, H.; André, S.; Tyteca, E.; Hubert, P. Supercritical Fluid Chromatography: A Promising Alternative to Current Bioanalytical Techniques. *Bioanalysis* **2018**, *10*, 107−124.

(12) Teubel, J.; Wüst, B.; Schipke, C. G.; Peters, O.; Parr, M. K. Methods in Endogenous Steroid Profiling − A Comparison of Gas Chromatography Mass Spectrometry (GC−MS) with Supercritical Fluid Chromatography Tandem Mass Spectrometry (SFC-MS/MS). *J. Chromatogr. A* **2018**, *1554*, 101−116.

(13) Zhang, X.; Ding, X.; Wang, J.; Dean, B. Supercritical Fluid Chromatography-Tandem Mass Spectrometry for High Throughput Bioanalysis of Small Molecules in Drug Discovery. *J. Pharm. Biomed. Anal.* **2019**, *164*, 62−69.

(14) Yang, Z.; Sun, L.; Liang, C.; Xu, Y.; Cao, J.; Yang, Y.; Gu, J. Simultaneous Quantitation of the Diastereoisomers of Scholarisine and 19-Epischolarisine, Vallesamine, and Picrinine in Rat Plasma by Supercritical Fluid Chromatography with Tandem Mass Spectrometry and Its Application to a Pharmacokinetic Study. *J. Sep. Sci.* **2016**, *39*, 2652−2660.

(15) Liu, M.; Zhao, L.; Yang, D.; Ma, J.; Wang, X.; Zhang, T. Preclinical Pharmacokinetic Evaluation of a New Formulation of a Bifendate Solid Dispersion Using a Supercritical Fluid Chromatography−Tandem Mass Spectrometry Method. *J. Pharm. Biomed. Anal.* **2014**, *100*, 387−392.

(16) Meng, X.; Yang, B.; Gao, J.; Peng, W.; Wang, H.; Shi, M.; Mortishire-Smith, R.; Yang, Y.; Gu, J. Simultaneous Quantitation of Two Diastereoisomers of Lobaplatin in Rat Plasma by Supercritical Fluid Chromatography with Tandem Mass Spectrometry and Its Application to a Pharmacokinetic Study. *J. Sep. Sci.* **2015**, *38*, 3803−3809.

(17) Humphries-Bickley, T.; Castillo-Pichardo, L.; Corujo-Carro, F.; Duconge, J.; Hernandez-O'Farrill, E.; Vlaar, C.; Rodriguez-Orengo, J. F.; Cubano, L.; Dharmawardhane, S. Pharmacokinetics of Rac Inhibitor EHop-016 in Mice by Ultra- Performance Liquid Chromatography Tandem Mass Spectrometry. *J. Chromatogr. B Anal. Technol. Biomed. Life Sci.* **2015**, *981−982*, 19−26.

(18) FDA US Department of Health and Human Services. Guidance for Industry: Bioanalytical Method Validation. http://www.fda.gov/downloads/Drugs/Guidances/ucm070107.pdf.

(19) Jin, Y.; Li, J.; Rong, L. F.; Lü, X. W.; Huang, Y.; Xu, S. Y. Pharmacokinetics and Tissue Distribution of 5-Fluorouracil Encapsu-

DOI: 10.1021/acsomega.9b01641
ACS Omega 2019, 4, 17981−17989

lated by Galactosylceramide Liposomes in Mice. *Acta Pharmacol. Sin.* **2005**, *26*, 250−256.
(20) Center for Drug Evaluation and Research. Pharmacology Review(s). Application Number: 22-059.
(21) O'Reilly, T.; McSheehy, P. M. J.; Kawai, R.; Kretz, O.; McMahon, L.; Brueggen, J.; Bruelisauer, A.; Gschwind, H. P.; Allegrini, P. R.; Lane, H. A. Comparative Pharmacokinetics of RAD001 (Everolimus) in Normal and Tumor-Bearing Rodents. *Cancer Chemother. Pharmacol.* **2010**, *65*, 625−639.
(22) Leighton, J.; Saber, H.; Lee, H. *Pharmacology Review-Everolimus*; Rockville, 2009.
(23) Sparreboom, A.; Van Tellingen, O.; Nooijen, W. J.; Beijnen, J. H. Preclinical Pharmacokinetics of Paclitaxel and Docetaxel. *Anticancer Drugs* **1998**, *9*, 1−17.
(24) Hampsch, R. A.; Shee, K.; Bates, D.; Lewis, L. D.; Désiré, L.; Leblond, B.; Demidenko, E.; Stefan, K.; Huang, Y. H.; Miller, T. W. Therapeutic Sensitivity to Rac GTPase Inhibition Requires Consequential Suppression of MTORC1, AKT, and MEK Signaling in Breast Cancer. *Oncotarget* **2017**, *8*, 21806−21817.
(25) Damsch, S.; Eichenbaum, G.; Tonelli, A.; Lammens, L.; Bulck, K. Van Den.; Feyen, B.; Vandenberghe, J.; Megens, A.; Knight, E.; Kelley, M. Gavage-Related Reflux in Rats:Identification, Pathogenesis, and Toxicological Implications (Review). *Toxicol. Pathol.* **2011**, *39*, 348−360.
(26) Hudachek, S. F.; Gustafson, D. L. Physiologically Based Pharmacokinetic Model of Lapatinib Developed in Mice and Scaled to Humans. *J. Pharmacokinet. Pharmacodyn.* **2013**, *40*, 157−176.
(27) Ooi, K.; Ohkubo, T.; Higashigawa, M.; Kawasaki, H.; Kakito, H.; Kagawa, Y.; Kojima, M.; Sakurai, M. Plasma, Intestine and Tumor Levels of 5-Fluorouracil in Mice Bearing L1210 Ascites Tumor Following Oral Administration of 5-Fluorouracil, UFT (Mixed Compound of Tegafur and Uracil), Carmofur and 5′-Deoxy-5-Fluorouridine. *Biol. Pharm. Bull.* **2001**, *24*, 1329−1331.
(28) Maldonado, M. del M.; Dharmawardhane, S. Targeting Rac and Cdc42 GTPases in Cancer. *Cancer Res.* **2018**, DOI: 10.1158/0008-5472.CAN-18-0619.
(29) Timmerman, P.; Mokrzycki, N.; Delrat, P.; De Meulder, M.; Erbach, E.; Lentheric, I.; McIntosh, M.; Dzygiel, P. Recommendations from the European Bioanalysis Forum on Method Establishment for Tissue Homogenates. *Bioanalysis* **2014**, *6*, 1647−1656.
(30) Wang, P.; Sun, J.; Xu, J.; Yan, Q.; Gao, E.; Qu, W.; Zhao, Y.; Yu, Z. Pharmacokinetics, Tissue Distribution and Excretion Study of Dictamnine, a Major Bioactive Component from the Root Bark of Dictamnus Dasycarpus Turcz. (Rutaceae). *J. Chromatogr. B* **2013**, *942*−*943*, 1−8.
(31) Wang, W.; Liu, J.; Zhao, X.; Peng, Y.; Wang, N.; Lee, D. Y. W.; Dai, R. Pharmacokinetics, Tissue Distribution, and Excretion Studies of l-Isocorypalmine Using Ultra High Performance Liquid Chromatography with Tandem Mass Spectrometry. *J. Sep. Sci.* **2017**, *40*, 1040−1048.
(32) The National Research Council Commitee for the Update of the Guide for the Care and Use of Laboratory Animals. In *Guide for the Care and Use of Laboratory Animals*, 8th ed.; National Academies Press: Washington, DC, 2011; Vol. *46*.
(33) Castillo-Pichardo, L.; Humphries-Bickley, T.; De La Parra, C.; Forestier-Roman, I.; Martinez-Ferrer, M.; Hernandez, E.; Vlaar, C.; Ferrer-Acosta, Y.; Washington, A. V.; Cubano, L. A.; Rodriguez-Orengo, J.; Dharmawardhane, S. The Rac Inhibitor EHop-016 Inhibits Mammary Tumor Growth and Metastasis in a Nude Mouse Model. *Transl. Oncol.* **2014**, *7*, 546−555.

DOI: 10.1021/acsomega.9b01641
ACS Omega 2019, 4, 17981−17989